First-principles phonon spectrum in bcc Ba: Three-ion forces and transition-metal behavior

John A. Moriarty
Lawrence Livermore National Laboratory, University of California, Livermore, California 94550
(Received 16 June 1986)

The influence of d electrons on the structural and vibrational properties of the heavy alkaline-earth metals increases with atomic number. The occurrence of the bcc structure in Ba (versus fcc in Ca and Sr) suggests the onset of transition-metal behavior, where the bottom of the $5d$ band has crossed below the Fermi level. This behavior also appears to be revealed in the recently measured phonon spectrum, which is found to be somewhat anomalous. We have made a first-principles analysis of the phonon spectrum of Ba in the context of the new transition-metal generalized pseudopotential theory. We find that partial filling of the $5d$ band is essential both to stabilize the bcc structure and to lower the calculated phonon frequencies into the measured range. Furthermore, the inclusion of three-ion angular forces (in addition to normal two-ion pair forces) is necessary to explain the observed anomalous lowering of the longitudinal branch below the transverse branch in the [100] direction.

I. INTRODUCTION

Our detailed understanding of the structural and vibrational properties of the heavy alkaline-earth metals has increased greatly in recent years through continued experimental[1-7] and first-principles theoretical[8-12] investigations. The theoretical studies have all pointed to the d bands in close proximity to the Fermi level as the main driving force for the richness in the observed properties. Furthermore, the influence of the d electrons on these properties increases rapidly both with atomic number at normal density and with pressure for a given element. At ambient conditions, it now appears that one already spans the full range of behavior from that of a near-ideal simple metal in Mg to that of an early transition metal in Ba. The latter behavior is revealed both through the observed bcc crystal structure (vs hcp in Mg and fcc in Ca and Sr) and through the recently measured phonon spectrum,[5,6] which in the most accurate single-crystal results[6] is found to have and an anomalous lowering of the longitudinal [100] branch below the transverse branch. Frozen-phonon calculations[12] at the midzone point in the [100] direction have confirmed that the latter is driven by the $5d$ electrons. In the present paper we attempt to further clarify the transition-metal behavior of Ba by considering a first-principles analysis of the entire phonon spectrum from a complementary point of view. In particular, we establish here the real-space central and angular forces which determine the phonons and the relationship of these forces to the partial d-band filling accompanying transition-metal behavior.

The importance of the d bands in the heavy alkaline-earth metals can be appreciated from Fig. 1, where we have plotted the central block features of the densities of states for Ca, Sr, and Ba. In Ca and Sr, the respective $3d$ and $4d$ bands reside close above the Fermi level E_F and their presence is felt through sp-d hybridization with the otherwise nearly-free-electron states at and below E_F. In Ba, on the other hand, the bottom of the $5d$ band has crossed below the Fermi level and not only is hybridization present but substantial filling of the $5d$ bands has also occurred. Self-consistent linear-muffin-tin-orbital (LMTO) calculations[10,13] indicate that there is nearly one d electron per atom in Ba at normal density, which amounts to 50% of the nominal valence of $Z=2$. In addition, for all three elements the d bands can be lowered with respect to E_F by the application of pressure, so that similar early transition-metal behavior can be induced in Ca and Sr as well. A clear fingerprint of this physics can be seen in the observed pattern[1,2] of crystal structures and transition pressures to the bcc phase, as summarized in Fig. 2. Here we include Mg and identify its hcp phase as the prototype simple-metal structure for the alkaline earths. In the absence of hybridization, this structure would also be maintained in Ca, as theoretical calculations have demonstrated.[8,14] Hybridization, however, stabilizes the fcc structure in Ca and Sr by introducing a dip in the density of states near E_F. The stabilization of the bcc structure in Ba and in Ca and Sr under pressure then closely correlates with the partial filling of the d bands as they are lowered below E_F and the onset of transition-metal behavior. The appearance of the bcc structure in Mg at high pressure is also driven by d-electron effects,[9] but the nature of the d bands in this case is sufficiently different that the correlation is less significant.

Our present analysis of the Ba phonon spectrum is based on the generalized pseudopotential theory (GPT), which we have previously developed for empty-d-band metals[8,14] (i.e., hybridization but no d-band filling) and have recently extended to include transition metals.[15] We have also recently applied a refined version of the empty-d-band GPT to the calculation of fcc phonons in Ca and Sr,[11] demonstrating that the electronic structure depicted in Fig. 1 is both qualitatively and quantitatively consistent with the observed phonon spectra. The challenge in this paper is to reconcile the more complex electronic structure of Ba with the observed behavior of the phonons. We

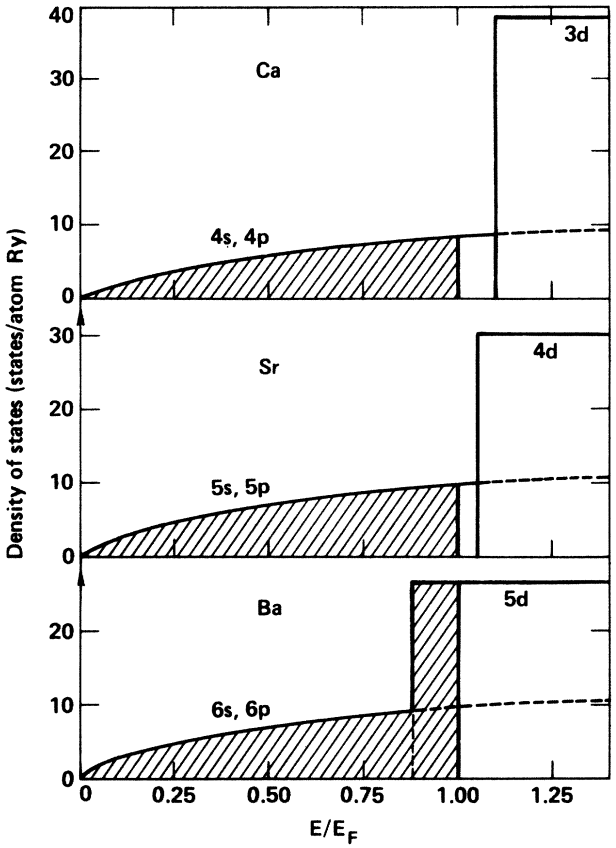

FIG. 1. Block features of the density of states in the heavy alkaline-earth metals. In each case the position of the d bands relative to the nearly-free-electron sp bands is shown, as determined by the present self-consistent LMTO calculations (Ref. 13). (The sp-d hybridization is not shown, but is included in the calculations.)

begin in Sec. II by discussing the GPT and its application to the problem at hand, including the determination of interatomic potentials for the alkaline-earth metals. Then in Sec. III, we consider the calculation of the phonon spectrum in the empty-d-band limit and contrast the striking success we find in Ca and Sr with the equally striking failure we obtain in the case of Ba. In Sec. IV, we analyze the Ba phonons in the transition-metal limit of the GPT, demonstrate the need for partial d-band filling to explain the observed spectrum, and attempt to elucidate the roles played by central and angular forces in this metal. We conclude in Sec. V.

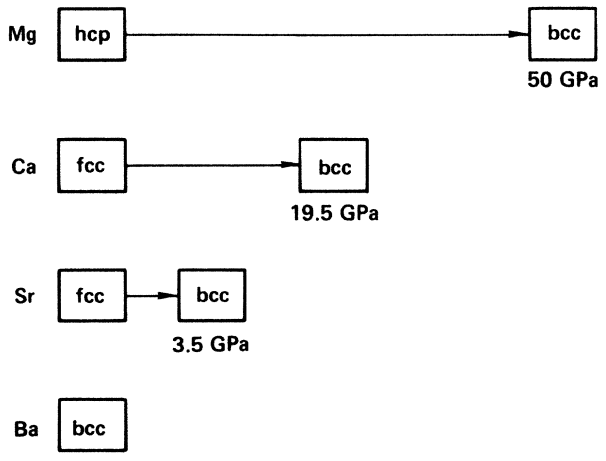

FIG. 2. Observed crystal structures and transition pressures to the bcc structure in the alkaline-earth metals (Refs. 1 and 2).

II. THEORETICAL FOUNDATIONS

The formal aspects of the GPT are discussed in detail in Refs. 14 and 15, where the theory is developed within the central framework of the first-principles Kohn-Sham local-density-functional formalism.[16] In the present work, as previously, we adopt the Hedin-Lundqvist exchange-correlation potential,[17] so that our starting point is essentially the same as in the frozen-phonon calculations of Chen *et al.*[12] The important distinguishing feature of the GPT is the expansion of the total energy in a multi-ion series valid for arbitrary atomic configurations in the bulk, in contrast to the nonperturbative determination of this quantity for highly symmetric atomic configurations with direct band-structure methods. In real space, the GPT total energy for a homogeneous, elemental metal with an atomic volume Ω takes the form

$$E_{\rm tot}(\mathbf{R}_1,\ldots\mathbf{R}_N)=E_0(\Omega)+\tfrac{1}{2}\sum_{i,j=1}^{N}{}' v_2(R_{ij}) + \tfrac{1}{6}\sum_{i,j,k=1}^{N}{}' v_3(R_{ij},R_{jk},R_{ki})+\cdots . \quad (1)$$

Here E_0 is a volume term and v_2, v_3, etc. are two-ion, three-ion, etc. interatomic potentials which are implicitly volume dependent, but explicitly *structure independent*, that is, they do not depend on the absolute ion coordinates $\mathbf{R}_i$ but only on relative ion separations $R_{ij}=|\mathbf{R}_i-\mathbf{R}_j|$, etc. and are thus completely *transferable* at fixed volume. Knowledge of the interatomic potentials permits the calculation of both total-energy differences among various structures and, for a given structure, the forces acting on the individual ions for arbitrary displacements from equilibrium.

The total-energy expansion in the GPT is carried out with a basis set of plane waves $|\mathbf{k}\rangle$ and localized, atomic-like d states $|\phi_d\rangle$. The quantities E_0, v_2, v_3, etc. in Eq. (1) are, in general, functionals of both a weak nonlocal pseudopotential w, through matrix elements $\langle\mathbf{k}'|w|\mathbf{k}\rangle$ and free-electron energies ε_k, and a weak hybridization potential Δ, through matrix elements $\langle\mathbf{k}|\Delta|\phi_d\rangle$ and $\langle\phi_d^i|\Delta|\phi_{d'}^j\rangle$, overlaps $\langle\mathbf{k}|\phi_d\rangle$ and $\langle\phi_d^i|\phi_{d'}^j\rangle$, and a mean d-state energy E_d. Setting $\Delta=\phi_d=0$ in the alkaline-earth metals corresponds to ignoring the d bands entirely, in which case our treatment reduces to a refined version of the usual pseudopotential perturbation theory. We refer to this as the simple-metal limit. In the empty-d-band limit, the hybridization is introduced perturbatively by noting that

$$\Delta^2/(E_d-\epsilon_k) \tag{2}$$

for $\epsilon_k \leq E_F$ is also a weak potential for expansion purposes, with the nominal valence of $Z=2$ for group-IIA elements being maintained. In the transition-metal limit, however, both of the latter constraints are relaxed. In place of Eq. (2), the expansion must be carried out in terms of the full relative d-state coupling strength, as defined in Ref. 15, with partial filling of the d bands taken into account. The valence Z, which physically is a measure of the number of s and p electrons per atom, is determined by a self-consistent procedure.[15] For Ba in the present work, we find $Z=1.25$, leaving $Z_d=0.75$ d electrons per atom, which is consistent with the LMTO band-structure calculations.[10,13]

The rapid convergence of the total-energy expansion (1) depends to a certain extent on the choice of d-basis state ϕ_d. In practice, ϕ_d is specified by the value of its logarithmic derivative D_2 at the atomic sphere radius R_a. While it is possible to apply general optimization criteria[14,15] to obtain D_2, our recent work on the Ca and Sr phonons[11] has suggested an even better procedure for the special case of the alkaline-earth metals. The latter involves fine-tuning D_2 so that the sensitive sp-d hybridized X_1 energy level for the fcc structure, as calculated in a one-plane-wave approximation in the GPT, exactly matches the corresponding result obtained in a fully-converged energy-band calculation. We have implemented this procedure here by performing parallel self-consistent LMTO calculations[13,18] on fcc Ca, Sr, and Ba and matching X_1-Γ_1 energy differences. It should be noted that this in no way compromises the first-principles integrity of the GPT since the resulting ϕ_d remains a rigorously allowable choice of basis state.

A complication arises in the case of Ba due to relativistic effects, which, although generally small and qualitatively unimportant, are not quantitatively negligible. The current formulation of the GPT is nonrelativistic, but our studies indicate that the major relativistic effect, namely, the lowering of s and p levels with respect to d levels, can be effectively absorbed into the theory by matching to a semirelativistic LMTO calculation of X_1-Γ_1 in the above procedure of determining ϕ_d. We have done this here and believe that it is adequate for present purposes, although a more refined treatment may be desirable in the future.

Figure 3 illustrates the two-ion pair potential $v_2(r)$ entering Eq. (1) for Ba, as determined in the simple-metal, empty-d-band, and transition-metal limits of the present GPT calculations.[19] All three results display similar qualitative features characteristic of the alkaline-earth metals: strong Coulomb repulsion at short distances, a negative well in the vicinity of near-neighbor distances, and low-amplitude Friedel oscillations at large distances. The major effect of both the sp-d hybridization and the partial d-band filling is to deepen the near-neighbor well and push its minimum to shorter distances, resulting in a more attractive potential. Note that the depth of the near-neighbor well increases by about a factor of 5 in proceeding from the simple-metal to the transition-metal limits.

In both simple metals and empty-d-band metals, the neglect of higher-order potentials beyond v_2 has proven to be a good approximation in most cases. In transition metals, on the other hand, the three-ion triplet potential v_3 can be of comparable importance to v_2, so it is of direct interest to retain v_3 in the transition-metal limit for Ba. The three-ion potential is here calculated as in Ref. 15, neglecting the weak s and p electron effects, but retaining a full treatment of the sp-d hybridization and d-band filling. In general, of course, v_3 is a three-dimensional function which depends on three distances or equivalently two distances and one angle. Figure 4 illustrates the angular dependence of v_3 for near-neighbor interactions in Ba. The particularly interesting thing to note about this potential is that it is completely attractive, which is in sharp contrast to the central Group VB and VIB bcc metals (e.g., V and Cr), where an entirely repulsive three-ion potential is found.[15] This is a d-band-filling effect associated with the oscillatory nature of the three-ion component of the density of states. At energies near the bottom of the d band, this component is positive, leading in the case of Ba to a net enhancement in state density near E_F (see Fig. 3 of Ref. 12), a lowering of the total energy, and an attractive v_3. For energies near the center of the d band, on the other hand, the three-ion component is negative, which raises the total energy and produces a repulsive v_3 in the central bcc metals. Both of these trends tend to be magnified as near neighbors are brought closer together, resulting in a strong angular dependence for v_3 at small angles, as seen in Fig. 4 with Ba. In this case, it should be noted that the rapidly increasing negative value of v_3 with decreasing angle below 60° is offset by a corresponding

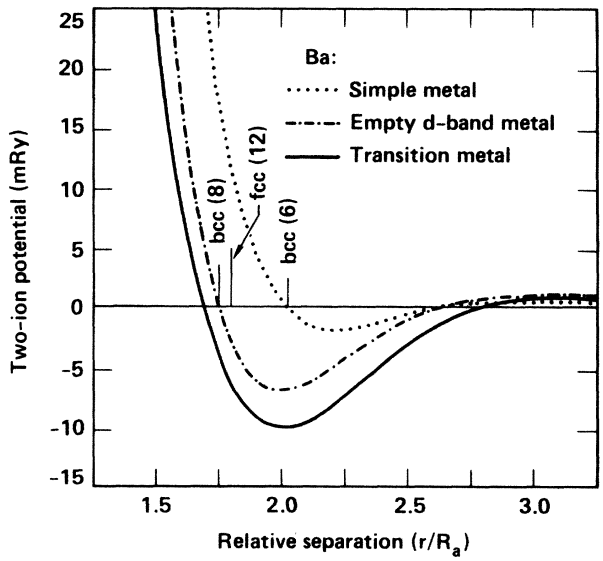

FIG. 3. Two-ion pair potential $v_2(r)$ in Ba, as obtained from the three limits of the present GPT calculations. The number and location of near neighbors in the fcc and bcc structures is indicated. The quantity R_a is the atomic-sphere radius.

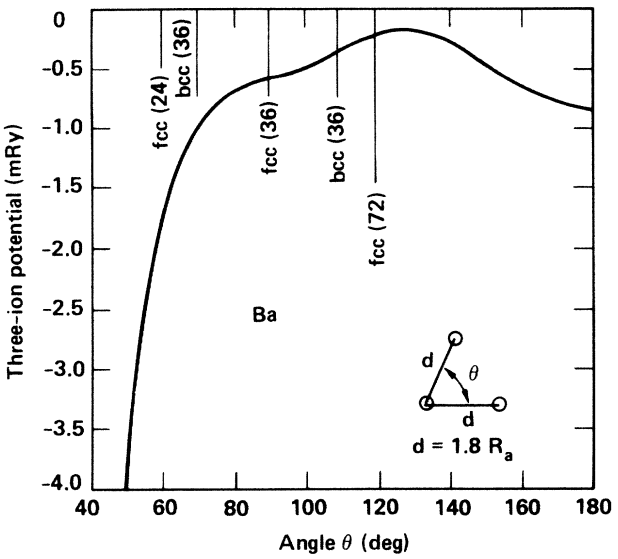

FIG. 4. Angular dependence of the three-ion triplet potential v_3 in Ba for near-neighbor interactions, as obtained in the transition-metal limit of the present GPT calculations. The number and location of three-ion triangles containing two nearest-neighbor distances in the fcc and bcc structures is indicated. The quantity R_a is the atomic-sphere radius.

rise in v_2, so that small-angle ion configurations are not energetically favorable. However, the large slope and curvature associated with the smallest bcc triangle does have important implications for the phonons, as we discuss below in Sec. IV.

III. PHONONS IN THE EMPTY-d-BAND LIMIT

A. Success for Ca and Sr

Before considering the central issue of the Ba phonons, we briefly discuss the results predicted for Ca and Sr in the empty-d-band limit of the GPT. We include Ca and Sr here both to update the calculations presented in Ref. 11 and to underscore the close connection of the structural and vibrational properties of the alkaline-earth metals to the d-band physics we have identified above. We have previously shown that the sp-d hybridization is essential for Ca and Sr both to stabilize the observed fcc structure[8,14] and to lower the phonon frequencies into close agreement with experiment.[11] The quantitative success of our present empty-d-band scheme[19,20] for these metals is demonstrated in Tables I and II. There we compare calculations of phase stability with self-consistent LMTO results[10] and elastic constants and phonon frequencies with experiment.[3–5] We include in Table II new experimental results recently published by Buchenau *et al.*[5] on Sr; these supersede the preliminary data of the same authors cited in Ref. 11.

The fcc phonon spectra of Ca and Sr display only weak anomalous behavior in the transverse T_1 branch in the [110] direction, and the observed softening[4,5] can be adequately explained by sp-d hybridization effects, as discussed in Ref. 11. Similarly, a recent measurement[7] of the high-temperature bcc phonon spectrum in Sr does *not* show the anomalous lowering of the longitudinal [100] branch below the transverse branch as seen in Ba. Additional empty-d-band GPT calculations on bcc Sr confirm

TABLE I. Structural and vibrational properties of fcc Ca, as obtained in the empty-d-band limit of the present GPT calculations. Included are total-energy differences (mRy), elastic constants (GPa), longitudinal (L) and transverse (T) zone-boundary phonon frequencies (THz), and the effective Debye temperature Θ_D (K).

	GPT	LMTO[a]	Experiment	
Phase stability:				
stable phase	fcc	fcc	fcc	
$E_{bcc}-E_{fcc}$	1.3	1.8		
$E_{hcp}-E_{fcc}$	0.8	0.5		
Elastic constants:				
C_{11}	30		25[b]	28[c]
C_{44}	18		20	16
$C_{11}-C_{12}$	10		10	10
Phonon frequencies:				
L[100]	5.0		4.9[b]	4.5[c]
T[100]	3.7		3.6	3.6
L[111]	4.8		4.8	4.6
T[111]	2.2		2.3	2.4
Θ_D[d]	211		210	207

[a]Reference 10.
[b]Reference 3 at 293 K.
[c]Reference 4 at 295 K. The elastic constants were determined from a force-constant fit to the measured phonon spectrum.
[d]As calculated from the Debye formula $E^0_{ph}=(9/8)k_B\Theta_D$, where E^0_{ph} is the actual zero-point vibrational energy.

TABLE II. Structural and vibrational properties of fcc Sr, as obtained in the empty-d-band limit of the present GPT calculations. Notation and units are the same as in Table I.

	GPT	LMTO[a]	Experiment	
Phase stability:				
stable phase	fcc	fcc	fcc	
$E_{bcc}-E_{fcc}$	1.8	0.8		
$E_{hcp}-E_{fcc}$	0.5	0.5		
Elastic constants:				
C_{11}	25		15[b,d]	16[c,d]
C_{44}	13		10	12
$C_{11}-C_{12}$	8		5	5
Phonon frequencies:				
L[100]	3.3		3.2[b]	3.2[c]
T[100]	2.4		2.3	2.2
L[111]	3.2		3.0	3.0
T[111]	1.4		1.4	1.4
Θ_D	137		131	129

[a]Reference 10.
[b]Reference 5 at 293 K.
[c]Reference 5 at 100 K.
[d]The C_{11} elastic constant was determined from the experimental bulk modulus of Ref. 23 and the measured value of $C_{11}-C_{12}$ via Eq. (6).

this result. All of the current evidence, therefore, points to the conclusion that the empty-d-band picture of Ca and Sr that we have developed is both necessary and sufficient to explain the structural and vibrational properties of these metals at normal density.

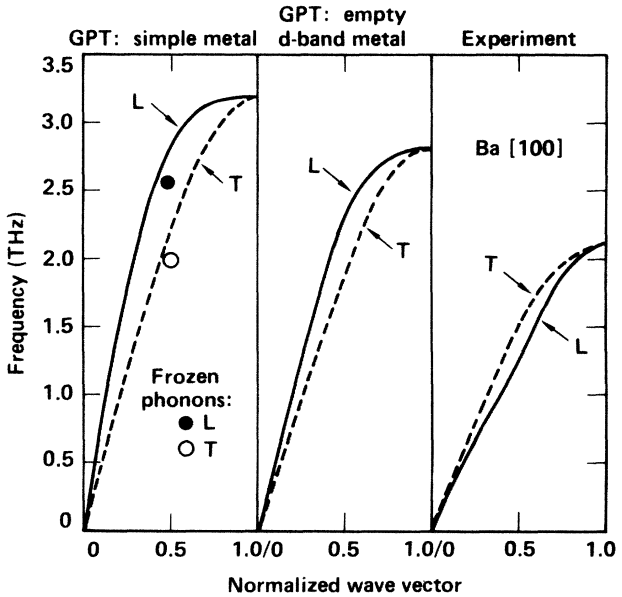

FIG. 5. Longitudinal (L) and transverse (T) [100] phonons in bcc Ba, as obtained in the simple-metal (left panel) and empty-d-band (center panel) limits of the present GPT calculations. The frozen-phonon results are those reported in Ref. 12 with the 5d bands removed to higher energy. The experimental curves (right panel) represent a force-constant fit to the measured frequencies in Ref. 6.

B. Failure for Ba

In the case of Ba, we have also investigated structural phase stability and the phonon spectrum in both the simple-metal and empty-d-band limits of the GPT. In the simple-metal limit, we find the fcc structure to have a slightly lower energy than either the hcp or bcc structures. The bcc structure remains mechanically stable, but its phonon frequencies lie about 50% above the measured values[5,6] with normal ordering of the longitudinal and transverse branches in the [100] direction, as shown in Fig. 5. At the midzone point in the [100] direction our results are nicely substantiated by the frozen phonon calculations of Chen *et al.*[12] performed with the 5d bands removed to higher energy. In the empty-d-band limit, the calculated phonon frequencies are lowered as expected, but only to within about 30% of experiment, as also shown in Fig. 5. The longitudinal and transverse [100] branches are moved slightly closer together, but display no tendency to cross. Even more seriously, the fcc structure is now more strongly stabilized and the bcc structure becomes mechanically unstable, with the entire T_1[110] branch found to have imaginary frequencies. Thus inclusion of the sp-d hybridization alone cannot satisfactorily explain the observed structural and vibrational properties of Ba.

IV. Ba PHONONS IN THE TRANSITION-METAL LIMIT

We now proceed to the transition-metal limit of the GPT and attempt to reconcile theory and experiment for Ba. We first consider the effect of pair forces alone by neglecting v_3 and higher-order potentials in Eq. (1). In this case, two out of the three major difficulties found

above in the empty-d-band limit are removed. First, the bcc structure is stabilized, with its total energy lowered below that of the fcc and hcp structures and all phonon frequencies found to be real, and second, the calculated frequencies are reduced to within 10% of experiment. The ordering of the [100] branches is not affected, however, as shown in Fig. 6. This latter outcome is furthermore not sensitive to the details of our calculation, but is, in fact, dictated by the general behavior of $v_2(r)$ shown in Fig. 3. The reason lies in the fact that, except at low wave number, the Ba phonons are dominated by the short-range forces of first- and second-neighbor interactions. By symmetry, first-neighbor forces alone lead to degenerate longitudinal and transverse [100] frequencies regardless of the interactions. This degeneracy is, however, lifted by the second-neighbor forces. The contribution of the latter to the longitudinal frequency squared ν_L^2 varies as the radial force constant

$$K_r \equiv \frac{d^2 v_2}{dr^2} , \tag{3}$$

and to the transverse frequency squared ν_T^2 as the tangential force constant

$$K_t \equiv \frac{1}{r}\frac{dv_2}{dr} , \tag{4}$$

with both derivatives evaluated at the second-neighbor distance. Clearly, one can have $\nu_T > \nu_L$, as found experimentally, if $K_t > K_r$. But inspection of Fig. 3 shows that this is very unlikely. The curvature K_r at the second-neighbor shell is positive in all cases, while the slope K_t is either near zero or negative. Thus $K_r > K_t$ and $\nu_L > \nu_T$ in all three limits of the GPT at the pair-potential level, in agreement with the results presented in Figs. 5 and 6.

The dilemma posed by the short-range behavior of v_2 is only removed when we permit the inclusion of angular forces through v_3. From inspection of Fig. 4, it can be appreciated that v_3 brings with it just the strong negative curvature need to reverse the positive second-neighbor $K_r - K_t$ value established by v_2. Indeed, as shown in Fig. 6, when three-ion forces are added in the present calculations,[21] the longitudinal [100] branch is lowered below the transverse branch in agreement with both experiment[6] and the frozen-phonon calculations of Chen *et al.*[12] In the process, the bcc structure remains both thermodynamically and mechanically stable and the phonon frequencies are further reduced in magnitude. The entire calculated phonon spectrum is compared with experiment in Fig. 7. On average, the calculated phonons with v_3 included now lie about 8% too low, but otherwise there is satisfactory overall agreement between theory and experiment. Note that the introduction of v_3 produces no further anomalous behavior in either the [110] or [111] directions.

An additional piece of evidence supporting the above picture is found in the more general correlation that exists between the behavior of the [100] phonons in bcc transition metals and the nature of v_3. Exactly as a purely attractive v_3 suppresses the [100] longitudinal phonons in Ba, a purely repulsive v_3, which is obtained in the Group VB and VIB metals, enhances these same phonons, pushing the longitudinal branch well above the transverse branch.[15] As is the case here, the latter behavior is essential to a proper explanation of the observed [100] spectra in metals such as V and Cr.

One aspect of the phonon spectrum of Ba which remains unresolved both experimentally and theoretically

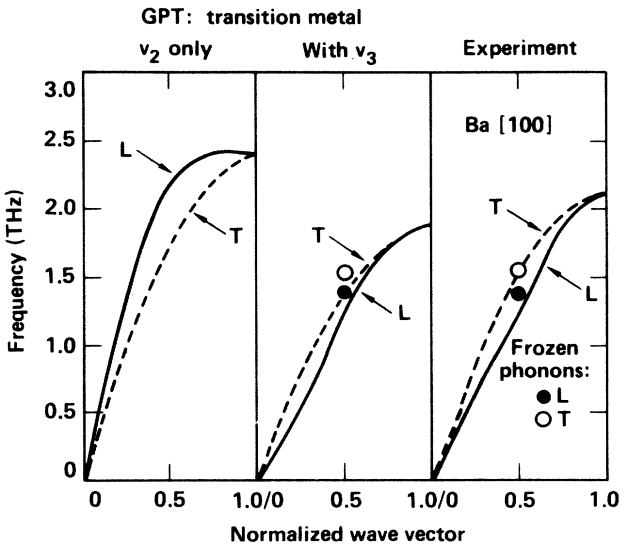

FIG. 6. Longitudinal (L) and transverse (T) [100] phonons in bcc Ba, as obtained in the transition-metal limit of the present GPT calculations. The left and center panels display the results calculated without and with the three-ion potential v_3, respectively. The frozen-phonon results are those reported in Ref. 12 with the $5d$ bands present. The experimental curves (right panel) are as in Fig. 5.

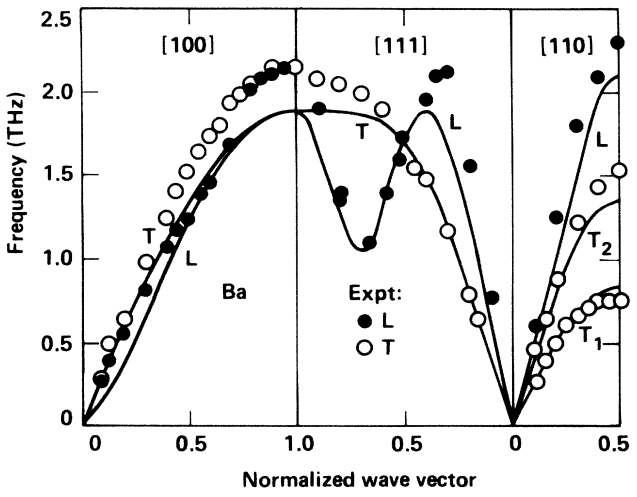

FIG. 7. Entire phonon spectrum in bcc Ba, as calculated in the transition-metal limit of the GPT including both pair (v_2) and triplet (v_3) interactions. The experimental data is from Ref. 6.

TABLE III. Summary of experimental elastic-constant data on bcc Ba. All values are in GPa.

Measurement	Buchenau *et al.*[a]		Mizuki *et al.*[b]	Other
Temperature (K)	100	293	295	~293
C_{44}	11.8±1.0	9.5±0.5	10.2	
$C_{11}-C_{12}$	5.4±0.4	4.6±0.2	6.6	
C_{11}		10.0±3.0	8.2	
C_{11} [Eq. (6)][c]	13.0	12.5	13.8	
B			3.7	9.4[d]; 10.5[e]

[a]Reference 5.
[b]Reference 6. Values are those inferred from the force-constant fit to the measured phonon spectrum (see Ref. 24).
[c]Calculated with $B=9.4$ GPa and the listed value of $C_{11}-C_{12}$.
[d]Reference 22.
[e]Reference 23.

concerns the very low-wave-number behavior of the longitudinal and transverse [100] branches and the corresponding C_{11} and C_{44} elastic constants. In addition to the single-crystal phonon data of Mizuki *et al.*,[6] there have been elastic-constant and phonon measurements on polycrystalline Ba reported by Buchenau *et al.*,[5] as well as direct compressibility measurements[22,23] yielding the bulk modulus. The sum total of experimental data relating to the Ba elastic constants is summarized in Table III, and from these results one can make a good circumstantial case that

$$C_{11} > C_{44} , \tag{5}$$

and hence that the longitudinal branch lies above the transverse branch at low wave number. This is seen most clearly by first writing

$$C_{11} = B + \tfrac{2}{3}(C_{11}-C_{12}) , \tag{6}$$

where B is the bulk modulus. Using the lowest directly measured values of B (9.4 GPa) and $C_{11}-C_{12}$ (4.6 GPa), one finds $C_{11}=12.5$ GPa, which is already above all reported values of C_{44}. In contrast, the value of $C_{11}=8.2$ GPa inferred by the force-constant fit to the data of Mizuki *et al.*[6] leads to an unrealistically low bulk modulus,[24] as shown in Table III. At the same time, apart from the behavior of the longitudinal [100] branch, the directly measured single-crystal phonon spectra[6] and the modeled polycrystalline phonon spectra[5] are in good overall agreement. The remaining discrepancy between the likely value of C_{11} and the single-crystal phonon frequencies could be resolved if there were a second anomaly in the [100] longitudinal branch which forced it back above the transverse branch at low wave number. We have, in fact, found some preliminary theoretical evidence for such behavior. While the present transition-metal GPT calculational scheme[21] necessarily suppresses the long-range tails of v_2 and v_3 for convergence reasons, we find that these tails do tend to produce the required anomaly when the range of interaction is allowed to increase. Unfortunately, the result does not converge in real space, and the actual form of the low-wave-number behavior must await the development of a corresponding reciprocal-space treatment.

V. CONCLUSIONS

In agreement with the frozen-phonon calculations of Chen *et al.*,[12] the present study points to the conclusion that bcc Ba behaves like an early transition metal, with the $5d$ bands partially occupied and strongly influencing the energetics of the individual ions. Unlike the cases of Ca and Sr, we find that weak *sp-d* hybridization alone *cannot* account for the observed structural and vibrational properties of this metal. In terms of the real-space picture of the total energy that has been developed here from the transition-metal GPT, the effect of the *d*-band filling is both to modify the central-force pair potential between ions and to introduce an angular-force triplet potential. We find that while the modified central forces alone can stabilize the bcc structure and lower the phonon frequencies into the observed range, the angular forces are necessary to properly account for the anomalous lowering of the longitudinal [100] branch below the transverse branch as seen in the single-crystal measurements of Mizuki *et al.*[6] One unresolved question that remains, both experimentally and theoretically, concerns the correct behavior of these [100] phonon branches at low wave number and the relative values of the corresponding C_{11} and C_{44} elastic constants. Additional experimental and theoretical work will be necessary to resolve this latter issue.

ACKNOWLEDGMENTS

The author wishes to thank Dr. A. K. McMahan for kindly providing the LMTO computer program used in part of the present research and Professor B. N. Harmon for sending a copy of Ref. 12 prior to publication and for a useful discussion. This work was performed under the auspices of the U.S. Department of Energy by Lawrence Livermore National Laboratory under Contract No. W-7405-Eng-48.

[1]H. Olijnyk and W. B. Holzapfel, Phys. Lett. **100A**, 191 (1984).
[2]H. Olijnyk and W. B. Holzapfel, Phys. Rev. B **31**, 4682 (1985).
[3]U. Buchenau, H. R. Schober, and R. Wagner, J. Phys. (Paris) Colloq. **42**, C6-395 (1981).
[4]C. Stassis, J. Zarestky, D. K. Mismer, H. L. Skriver, B. N. Harmon, and R. M. Nicklow, Phys. Rev. B **27**, 3303 (1983).
[5]U. Buchenau, M. Heiroth, H. R. Schober, J. Evers, and G. Oehlinger, Phys. Rev. B **30**, 3502 (1984).
[6]J. Mizuki, Y. Chen, K.-M. Ho, and C. Stassis, Phys. Rev. B **32**, 666 (1985).
[7]J. Mizuki and C. Stassis, Phys. Rev. B **32**, 8372 (1985).
[8]J. A. Moriarty, Phys. Rev. B **8**, 1338 (1973); **6**, 4445 (1972).
[9]J. A. Moriarty and A. K. McMahan, Phys. Rev. Lett. **48**, 809 (1982); A. K. McMahan and J. A. Moriarty, Phys. Rev. B **27**, 3235 (1983).
[10]H. L. Skriver, Phys. Rev. Lett. **49**, 1768 (1982); Phys. Rev. B **31**, 1909 (1985).
[11]J. A. Moriarty, Phys. Rev. B **28**, 4818 (1983).
[12]Y. Chen, K.-M. Ho, B. N. Harmon, and C. Stassis, Phys. Rev. B **33**, 3684 (1986).
[13]The present self-consistent LMTO band-structure calculations have been carried out for fcc Ca, Sr, and Ba within the Kohn-Sham local-density framework (Ref. 16), using the Hedin-Lundqvist exchange-correlation potential (Ref. 17). The calculations employ the atomic-sphere approximation, the combined-correction term to this approximation, and s, p, d, and f angular momentum components (Ref. 18). A semirelativistic treatment has been used in the case of Ba, while in Ca and Sr the calculations have been done nonrelativistically. For Ba we obtain 0.875 d electrons per atom.
[14]J. A. Moriarty, Phys. Rev. B **26**, 1754 (1982); **16**, 2537 (1977).
[15]J. A. Moriarty, Phys. Rev. Lett. **55**, 1502 (1985) and unpublished.
[16]W. Kohn and L. J. Sham, Phys. Rev. **140**, A1133 (1965).
[17]L. Hedin and B. I. Lundqvist, J. Phys. C **4**, 2064 (1971).
[18]H. L. Skriver, *The LMTO Method* (Springer, Berlin, 1984).
[19]In addition to our new procedure for choosing the basis d state ϕ_d, the present calculations use the analytic form developed by S. Ichimaru and K. Utsumi, Phys. Rev. B **24**, 7385 (1981) for the exchange-correlation function $G(q)$ entering the electron screening. The present $G(q)$, however, is still based on the Hedin-Lundqvist exchange and correlation energy (Ref. 17) and results in only small changes for the alkaline-earth metals from our previous treatment (Refs. 11 and 14).
[20]The GPT results presented in Tables I and II and in Fig. 5 were obtained at the pair potential level of Eq. (1), i.e., neglecting higher-order potentials beyond v_2. In Tables I and II, the values given for the structural energy differences and elastic constants, which depend on very long-range real-space interactions, were calculated from an exactly equivalent reciprocal-space formalism (Ref. 14).
[21]The transition-metal GPT calculations presented in Figs. 6 and 7 were carried out entirely in real space, with the long-range hybridization tails of v_2 and v_3 damped in the manner described in Ref. 15. The latter damping affects only the very low-wave-number phonons to any important degree, but does preclude an accurate treatment of the elastic constants in Ba, especially C_{11}.
[22]S. N. Vaidya and G. C. Kennedy, J. Phys. Chem. Solids **31**, 2329 (1970).
[23]K. A. Gschneidner, Solid State Phys. **16**, 275 (1964).
[24]We find a minor disagreement between the $C_{11}-C_{12}$ elastic constant we calculate from the force-constant data in Table II of Ref. 6 and the value given in that table. While we reproduce the listed values of C_{11} and C_{44} (as well as the plotted phonon spectrum in Fig. 3 of Ref. 6), we find $C_{11}-C_{12}=6.6$ GPa as opposed to the value of 8.5 GPa inferred from Table II. Our value improves the agreement with Ref. 5 for this result.